

Vibration Isolation of Magnetic Suspended Platform with Double Closed-loop PID Control

Mao Tang¹, Jin Zhou¹, Chaowu Jin¹, and Yuanping Xu^{1,2}

¹College of Mechanical and Electrical Engineering
Nanjing University of Aeronautics and Astronautics, Nanjing 210016, China
tangm@nuaa.edu.cn, zhj@nuaa.edu.cn, jinchaowu@nuaa.edu.cn, ypxu@nuaa.edu.cn

²Laboratory of Robotic Systems
Ecole Polytechnique Federale Lausanne (EPFL), Lausanne 1015, Switzerland

Abstract — In magnetic vibration isolation field, magnetic force is used for the isolation, while the whole isolation system is always supported passively, which have non-control shortcomings. Aimed at this problem, a novel active control strategy with a double closed-loop PID algorithm was designed in this paper. The double closed-loop strategy includes an internal and external loop control, which was designed to fulfill the magnetic levitation and isolation, respectively. Firstly, the vibration isolation strategy proposed in this paper was simulated in both time and frequency domain. The simulation results showed that this method possesses good performance of vibration isolation. Then, an active levitation and vibration isolation control experiment was designed. The experimental results showed that the control algorithm has a good vibration control effect under periodic vibration and random vibration conditions.

Index Terms — Double closed-loop PID, magnetic levitation, vibration isolation.

I. INTRODUCTION

With the development of precise and ultraprecise manufacturing technology, the vibration control in the process of mechanical equipment operation is getting more and more attention. The research on the vibration isolation control has developed from passive isolation control to active isolation control [1-2], and from single degree-of-freedom (DOF) vibration [3-4] to multi degrees-of-freedom vibration [5-6].

The magnetic levitation technology possesses the advantages of no contact, no friction, free of lubricating oil pollution, adjustable bearing stiffness and levitation position [7]. Thus, the application of vibration control combining with the magnetic levitation technology has good prospects.

For most of the magnetic vibration isolation system, the whole system is supported by the traditional methods

such as spring, rubber pad and air bag [3, 6, 8]. Although traditional passive support can bear more weight, the bearing characteristics like height and stiffness are not easy to adjust. And traditional passive support is unable to achieve active control to the external disturbance. Therefore, the magnetic technology can be utilized to support and isolate vibration using the electromagnetic force without any additional vibration isolation equipment, which is very promising for the optical instruments, or those light load equipment sensitive to vibration. This method can simplify the vibration isolation system structure, reduce cost, and increase the vibration isolation frequency range combining the passive and active vibration isolation. So the magnetic suspension platform realizing both stable suspension and broadband vibration isolation has great research value.

In this paper, a new double closed-loop control based on the PID control [9] was proposed and applied to a one DOF magnetic levitation platform with the combined functions of active levitation and the active vibration isolation. The controller using the relative displacement and absolute acceleration as feedback signal adopted the inner loop to control the magnetic levitation support and the outer one to control the vibration isolation.

The remainder of this paper is organized as follows: Section 2 analyzes the vibrating transmissibility of the passive vibration isolation system and the passive-active vibration isolation system. Section 3 presents the vibrating transmissibility of magnetic levitation system with inner PID loop controlling the magnetic levitation support. Section 4 is the simulation of the system with double closed-loop PID. Section 5 shows the experimental results of the magnetic levitation system with double closed-loop PID control, and conclusion are drawn in Section 6.

II. ACTIVE AND PASSIVE VIBRATION ISOLATION

According to whether the controller is needed or not,

vibration isolation system can be divided into active and passive vibration isolation system. Passive vibration isolation system can be simplified as one DOF mass-spring-damping vibration isolation model, as shown in Fig. 1.

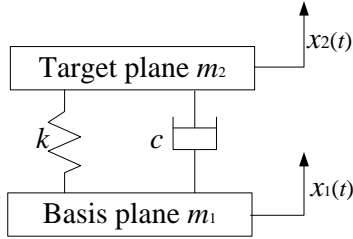


Fig. 1. Principle for passive isolation.

For the Fig. 1, the equation of motion can be written as:

$$m_2 \ddot{x}_2(t) + k(x_2(t) - x_1(t)) + c(\dot{x}_2(t) - \dot{x}_1(t)) = 0, \quad (1)$$

where m_2 is the mass of the target plane, k is the supporting stiffness, c is the damping coefficient, $x_1(t)$ is vibration displacement of the basis plane, and $x_2(t)$ is the vibration displacement of the target plane. The main purpose of the vibration isolation is to reduce the vibration transmitted from the basic object to the target plane.

The transmissibility of vibration acceleration amplitude is:

$$\frac{\ddot{X}_2}{\ddot{X}_1} = \frac{X_2}{X_1} = \sqrt{\frac{k^2 + (c\omega)^2}{(k - m_2\omega^2) + (c\omega)^2}}, \quad (2)$$

where X_1 and X_2 are amplitude of the basis plane and the amplitude of the of the target plane, respectively. ω is the frequency of vibration. Therefore, the relationship between the vibration frequency and the vibration transmissibility can be obtained:

$$\begin{cases} \frac{\ddot{X}_2}{\ddot{X}_1} \geq 1, \omega \leq \sqrt{\frac{2k}{m_2}} = \sqrt{2}\omega_n \\ \frac{\ddot{X}_2}{\ddot{X}_1} < 1, \omega > \sqrt{\frac{2k}{m_2}} = \sqrt{2}\omega_n \end{cases}, \quad (3)$$

where ω_n is the natural frequency of vibration without damping. According to Equation (3), the passive vibration isolation is effective only when the vibration frequency ω is larger than $\sqrt{2}\omega_n$. This limitation restricts the application of passive vibration isolation in low frequency vibration.

With the development of control technology, active vibration isolation becomes more and more important and relatively has better performance in theory comparing to the passive isolation. In order to combine the advantages of passive vibration isolation with the advantages of active vibration isolation, active isolator can be series connected with the passive vibration

isolation, which is shown in Fig. 2.

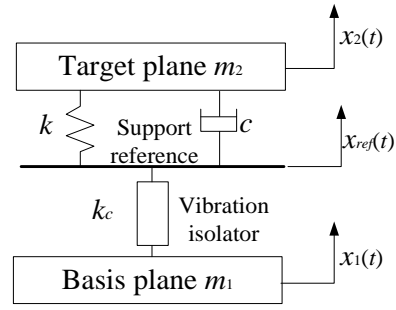


Fig. 2. Principle for series connection of passive isolation and active isolation.

The active vibration isolation uses the acceleration signal of the target plane as the feedback signal. Then, the vibration isolation controller outputs the control signal to change relative position between x_1 and the support reference position x_{ref} . The control function is:

$$x_{ref} - x_1 = K_c \ddot{x}_2, \quad (4)$$

where K_c is the active controller transfer function. The motion equation of the whole system is:

$$\begin{cases} m_2 \ddot{x}_2 + k(x_2 - x_{ref}) + c(\dot{x}_2 - \dot{x}_{ref}) = 0 \\ x_{ref} - x_1 = K_c \ddot{x}_2 \end{cases}. \quad (5)$$

In order to simplify the analysis, we assume that the control transfer function K_c is the constant gain k_c . The vibration acceleration amplitude transmissibility with the active vibration isolator is:

$$\frac{\ddot{x}_2}{\ddot{x}_1} = \frac{x_2}{x_1} \quad (6)$$

$$= \sqrt{\frac{k^2 + (c\omega)^2}{[-(m_2 - k k_c)\omega^2 + k] + (c\omega + c k_c \omega^3)^2}}.$$

The effect of vibration isolation is expressed by the logarithm of the transmissibility:

$$\lambda = 20 \log_{10} \frac{\ddot{X}_2}{\ddot{X}_1}. \quad (7)$$

Figure 3 draws the vibration transmissibility for passive isolation with and without active isolation series connected.

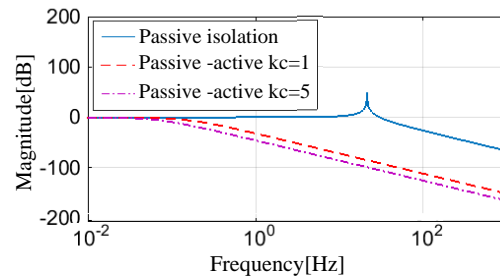


Fig. 3. Comparison of vibration transmissibility between the passive isolation with and without active isolation series connected.

In Fig. 3, compared to passive vibration isolation, resonance frequency and resonance peak decrease with vibration active isolator series connected. Logarithmic transmissibility of vibration acceleration is less than 0 at low frequency. And when k_c is larger, the vibration transmissibility is lower.

III. MAGNETIC LEVITATION PLATFORM

Magnetic levitation system is composed of controller, power amplifier, displacement sensors, acceleration sensor, soft magnetic material and coil, as shown in Fig. 4. The displacement signal of target plane measured by the displacement sensor is used as a feedback signal to be input to the controller. The control signal is converted into the control current i through a power amplifier, which is superimposed with the bias current I , and input to the coil. Then the electromagnet generates electromagnetic force to the suspended target plane, in order to control movement of the target plane.

The mathematical model of 1-DOF magnetic levitation platform is:

$$m\ddot{x} + mg = F(x, i), \quad (8)$$

where m is the total mass of suspended target which contains target plane and thrust disc and shaft between them as shown in Fig. 4, \ddot{x} is the acceleration of the levitation target, F is electromagnetic force resultant from the upper and lower magnetic poles, and x is the displacement compared to the middle position.

At the equilibrium position, the linearized electromagnetic force $F(x, i)$ can be written as [10]:

$$\hat{F}(x, i) = k_i \cdot i + k_x \cdot x, \quad (9)$$

where k_i and k_x are the open loop current gain and the actuator stiffness, respectively.

The control block diagram of the magnetic levitation supporting system is shown in Fig. 5.

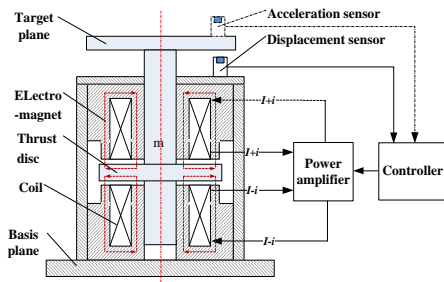


Fig. 4. 1-DOF magnetic levitation platform.

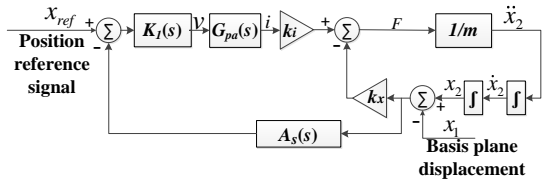


Fig. 5. Diagram of magnetic levitation supporting system.

Figure 5 presents the magnetic levitation supporting system based on PID control. $K_1(s)$ is the support controller with PID control, $G_{pa}(s)$ is the transfer function of the power amplifier, $A_s(s)$ is the displacement sensor, x_{ref} is position reference signal. x_2 is absolute displacement of the target plane. x_1 is the basis plane absolute displacement. The input of magnetic support system is the acceleration signal of basis plane. And the output of magnetic support system is the acceleration signal of target plane. The transfer function is:

$$\frac{\ddot{x}_2(s)}{\ddot{x}_1(s)} = \frac{A_s(s)K_1(s)G_{pa}(s)k_i + k_x}{ms^2 + A_s(s)K_1(s)G_{pa}(s)k_i + k_x}. \quad (10)$$

$G_1(s) = A_s(s)K_1(s)G_{pa}(s)k_i + k_x$, $s = j\omega$, so the vibration transmissibility is:

$$\frac{\ddot{X}_2}{\ddot{X}_1} = \sqrt{\frac{\text{Re}^2(G_1(j\omega)) + \text{Im}^2(G_1(j\omega))}{[\text{Re}(G_1(j\omega)) - m_2\omega^2]^2 + \text{Im}^2(G_1(j\omega))}}. \quad (11)$$

The transfer function of the PID control can be written as:

$$K_j(s) = K_{p,j} \left(1 + \frac{1}{T_{i,j}s} + \frac{T_{d,j}}{1+T_{f,j}s} s \right) \quad (12)$$

$$= P_j + I_j \frac{1}{s} + \frac{D_j}{1+T_{f,j}s} s,$$

where $j = 1, 2$, $P_j = K_{p,j}$ is proportion coefficient, $I_j = K_{p,j}/T_{i,j}$ is integral coefficient, and $D_j = K_{p,j}T_{d,j}$ is differential coefficient, and $T_{f,j}$ is the time constant of the low-pass filter.

Using three different PID control parameter groups, the vibration acceleration transmissibility of magnetic support system is simulated without vibration isolator. The simulation results show in Fig. 6.

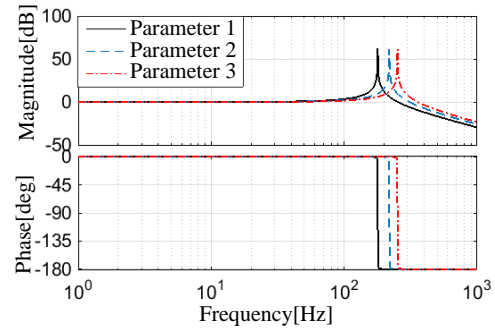


Fig. 6. Simulated vibration transmissibility of levitation supporting loop with different control parameters.

The three PID parameter groups (parameter 1, parameter 2 and parameter 3) have different value of proportion coefficient and integral coefficient and differential coefficient respectively. According to the simulation results, the levitation support system has the effect of vibration isolation only in the high frequencies, while the vibration that transmitted to the target plane

will be amplified in the lower frequencies. The vibration transmission characteristics are similar to the passive vibration isolation system.

IV. NUMERICAL SIMULATIONS FOR DOUBLE CLOSED-LOOP PID

To realize active supporting and active vibration isolation at the same time with only one magnetic levitation actuator, the controller needs new control strategy. The control system contains the active vibration isolation loop and the levitation support loop. For the vibration isolation, in order to facilitate the installation of sensors and vibration signal measurement, the acceleration sensor is used to measure the target plane vibration. For the levitation support, displacement sensor is used to measure the relative displacement of the target plane relative to the basis plane.

Figure 7 is the control system block diagram in which the inner loop is nested in the outer loop. In the outer loop, \ddot{x}_2 is the acceleration signal of the target plane measured by acceleration sensor, $A_a(s)$ is the transfer function of acceleration sensor. $K_2(s)$ is the isolation controller. The output signal of $K_2(s)$ which is the position reference signal x_{ref} of the inner levitation support loop, is input to the levitation support controller $K_1(s)$. The control signal from $K_1(s)$ is transformed into control current by power amplifier to control the target plane.

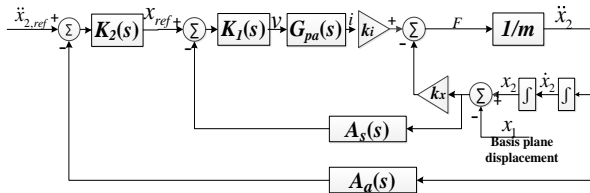


Fig. 7. Diagram for internal-and-external loop control system.

Vibration isolation controller $K_2(s)$ also uses the PID control. The structure of the system can be equivalent to the system shown in the Fig. 2.

After adding the isolation loop, transfer function from the basis acceleration \ddot{x}_1 to the target acceleration \ddot{x}_2 is:

$$\frac{\ddot{x}_2(s)}{\ddot{x}_1(s)} = \frac{A_a(s)K_1(s)G_{pa}(s)k_i + k_x}{ms^2 + A_s(s)K_1(s)G_{pa}(s)k_i + k_x + A_a(s)K_1(s)K_2(s)G_{pa}(s)k_i s^2} \quad (13)$$

$G_2(s) = A_a(s)K_1(s)G_{pa}(s)k_i s^2$, $s = j\omega$, so the vibration transmissibility is:

$$\frac{\ddot{X}_2}{\ddot{X}_1} = \sqrt{\frac{\text{Re}^2(G_1(j\omega)) + \text{Im}^2(G_1(j\omega))}{[\text{Re}(G_1(j\omega)) + \text{Re}(G_2(j\omega)) - m_2\omega^2]^2 + [\text{Im}(G_1(j\omega)) + \text{Im}(G_2(j\omega))]^2}} \quad (14)$$

The acceleration sensor transfer function is:

$$A_a = A_g \times 0.0078, \quad (15)$$

where A_g is the acceleration signal gain. The vibration transmissibility at different A_g shows in Fig. 8.

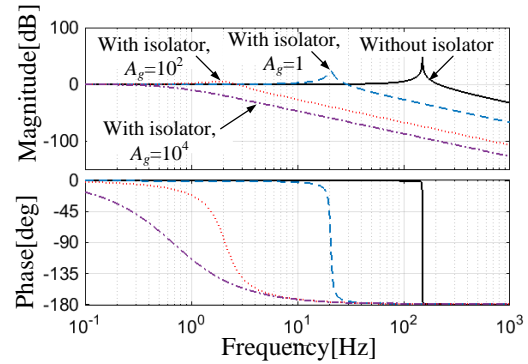


Fig. 8. Comparison among the simulated vibration transmissibility with different A_g .

As Fig. 8 shows, the addition of active vibration isolation loop can effectively reduce the vibration transmissibility and the resonance frequency.

After adding the active vibration isolation loop, the dynamic characteristics of new system is obtained through the step response simulation. The result shows in Fig. 9.

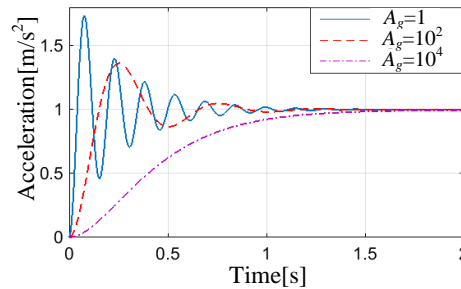


Fig. 9. Step response of double closed-loop PID control system with different A_g .

Figure 9 is the system step response at different A_g , when adding vibration isolation loop. It can be seen from the figure, with the increase of A_g , the overshoot decreases and the settling time increases. So when A_g ranging from 100 to 300, the system can get better performance.

The vibration isolation effect of the system is simulated in time domain, taking $A_g=10$, with the vibration acceleration amplitude of basis plane is 1.0m/s^2 and vibration frequency is 25 Hz. Amplitude of target plane with and without the isolation shows in Fig. 10. Without the vibration isolation, the vibration amplitude of the target plane is 1.0m/s^2 , while with the vibration isolation, the amplitude becomes 0.08m/s^2 . So the amplitude transmissibility is -21.9 dB.

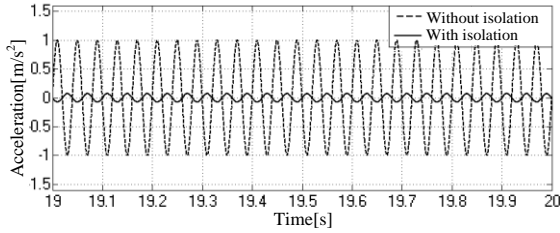


Fig. 10. Simulated result in time domain, 25 Hz.

When the basis plane vibrates randomly with maximum amplitude of 1.0m/s^2 , it can be seen from the Fig. 11 that, without vibration isolation loop, maximum amplitude of levitation target is magnified and about 5.5m/s^2 . With the vibration isolation loop, the maximum amplitude of target plane is 0.6m/s^2 , so isolation effect to the random vibration is equally obvious.

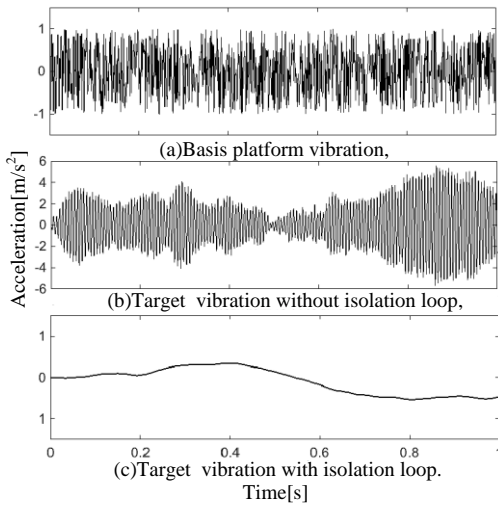


Fig. 11. Simulated results in time domain of random vibration isolation.

V. VIBRATION ISOLATION EXPERIMENT

The principle diagram of the experimental magnetic levitation platform with active vibration isolation and levitation support is shown in Fig. 12. And the real experimental system built according to principle diagram consisting of seven main parts is shown in Fig. 13.

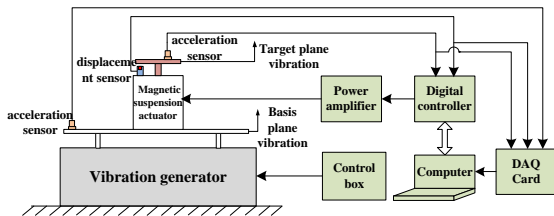


Fig. 12. Vibration isolation with double closed-loop PID control.

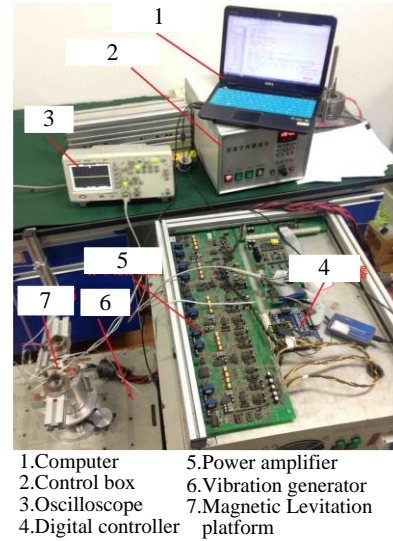


Fig. 13. Real experimental equipment.

Setting vibration frequency of the basis plane to 25 Hz, for the convenience of observation, using acceleration sensor to detect the vibration signal, the vibration acceleration with and without vibration isolation loop is compared in Fig. 14 and Fig. 15. The vibration acceleration amplitude of the basis plane is 10.1m/s^2 . Without the vibration isolation loop, the target vibration acceleration is amplified to 13.2m/s^2 . After adding vibration isolation loop, the amplitude of acceleration is 3.33m/s^2 . The vibration acceleration transmissibility from the basis to the target plane before and after adding the vibration isolation loop is respectively 2.33 dB and -9.46 dB.

As shown in the Fig. 16, after the vibration isolation, the power density of the basic frequency 24.9 Hz and the double frequency 49.8 Hz of the target plane respectively reduce 71.4% and 93.3%.

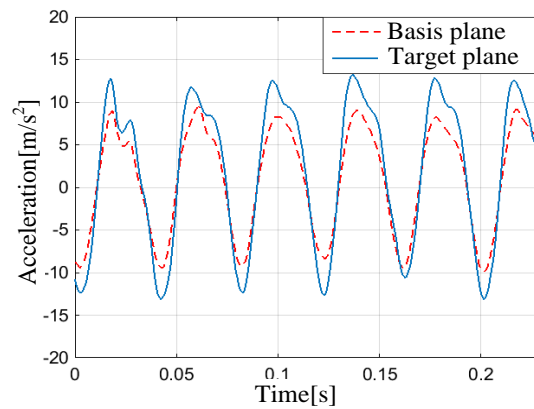


Fig. 14. Experimental comparison between base plane and target plane vibration without vibration isolation loop, 25 Hz.

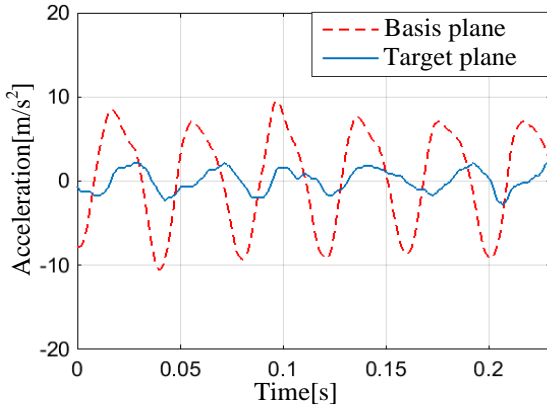


Fig. 15. Experimental comparison between base plane and target plane vibration with vibration isolation loop, 25 Hz.

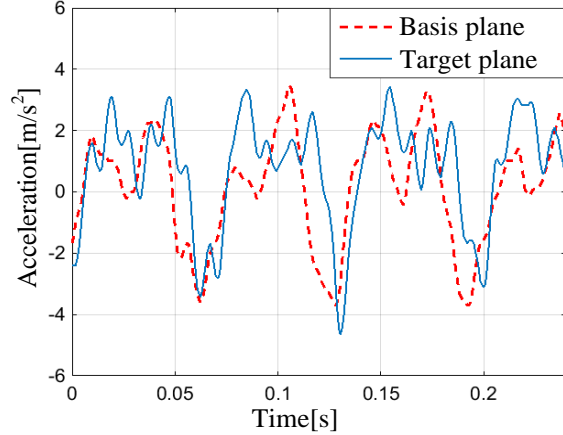


Fig. 17. Experimental comparison between base plane and target plane vibration without vibration isolation loop, random vibration.

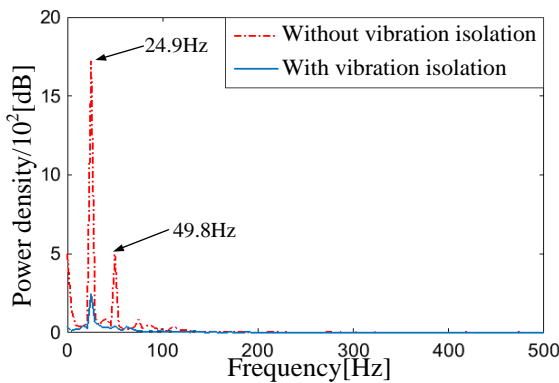


Fig. 16. Experimental spectrogram of frequency domain.

Setting the basis plane vibration to random vibration which has lower frequency components, the comparison between the acceleration without and with the vibration isolation is shown as Figs. 17 and 18. Without the isolation loop, vibration amplitude of the basis plane acceleration is 3.59m/s^2 and the amplitude of the target acceleration is 4.10m/s^2 . And after adding isolation loop, vibration amplitude of the basis plane acceleration is 4.15m/s^2 and the amplitude of the target acceleration is 1.84m/s^2 . The vibration acceleration transmissibility from the basis plane to the target plane without and with the vibration isolation is respectively 1.15 dB and -7.06 dB. So the target vibration acceleration is obviously reduced relative to acceleration without the isolation.

From Fig. 19, in the power density of random vibration, the main frequency components after the vibration isolation have a significant reduction in. Such as in 14.8 Hz frequency, the power density decreases by 55.1% and in 29.1 Hz frequency, the power density decreases by 75.9%.

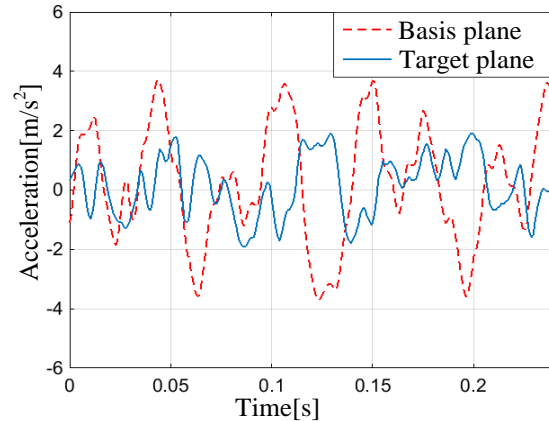


Fig. 18. Experimental comparison between base plane and target plane vibration with vibration isolation loop, random vibration.

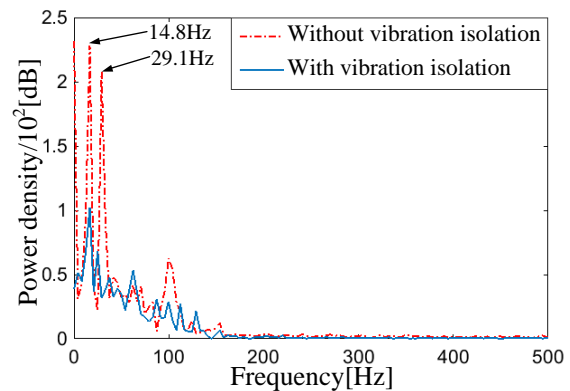


Fig. 19. Experimental spectrogram of frequency domain of random vibration.

VI. CONCLUSION

This paper proposed a new double closed-loop vibration isolation strategy which contained inner loop for levitation support and outer loop for vibration isolation. The double closed-loop control system was designed for the magnetic levitation platform. The simulation result shows the good vibration isolation effect of this method. And the bigger the acceleration sensor gain A_g is, the better the vibration isolation effect is. The vibration isolation experiment of magnetic levitation vibration isolation system with double closed-loop PID control under periodic and random vibration conditions was designed to prove the effectiveness of vibration isolation. After adding the vibration isolation loop, vibration acceleration transmissibility of 25 Hz periodic vibration decreased from 2.33 dB to -9.46 dB. And the maximum acceleration transmissibility of low frequency random vibration decreased from 1.15 dB to -7.06 dB.

ACKNOWLEDGMENT

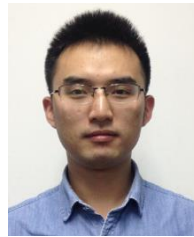
This work was supported by the National Natural Science Foundation of China (51675261), and the Fundamental Research Funds for the Central Universities (NS2016053), and the Open Project Program of Jiangsu Key Laboratory of Large Engineering Equipment Detection and Control (JSKLEDC201502).

REFERENCES

- [1] D. L. Margolis, "A procedure for comparing passive, active, and semi-active approaches to vibration isolation," *Journal of the Franklin Institute*, vol. 315, no. 4, pp. 225-238, 1983.
- [2] L. L. Sun, C. H. Hansen, and C. Doolan, "Evaluation of the performance of a passive-active vibration isolation system," *Mechanical Systems & Signal Processing*, vol. 50-51, pp. 480-497, 2015.
- [3] Y. B. Kim, W. G. Hwang, C. D. Kee, and H. B. Yi, "Active vibration control of a levitation system using an electromagnetic damper," *Proceedings of the Institution of Mechanical Engineers Part D Journal of Automobile Engineering*, vol. 215, pp. 865-873, 2001.
- [4] F. An, H. Sun, and X. Li, "Adaptive active control of periodic vibration using maglev actuators," *Journal of Sound and Vibration*, vol. 331, no. 9, pp. 1971-1984, 2012.
- [5] B. de Marneffe, M. Avraam, A. Deraemaeker, M. Horodinca, and A. Preumont, "Vibration isolation of precision payloads: a six-axis electromagnetic relaxation isolator," *Journal of Guidance Control and Dynamics*, vol. 32, no. 2, pp. 395-401, 2009.
- [6] Y. Kim, S. Kim, and K. Park, "Magnetic force driven six degree-of-freedom active vibration isolation system using a phase compensated velocity

sensor," *Review of Scientific Instruments*, vol. 80, no. 11, pp. 1347-1352, 2009.

- [7] Y. Xu, J. Zhou, C. Jin, and Q. Guo, "Identification of the dynamic parameters of active magnetic bearings based on the transfer matrix model updating method," *Journal of Mechanical Science & Technology*, vol. 30, no. 7, pp. 2971-2979, 2016.
- [8] C. Song, Y. Hu, and Z. Zhou, "Control mechanism of a differential magnetic levitation active vibration isolation system," *Journal of Vibration and Shock*, vol. 29, no. 7, pp. 24-27, 2010.
- [9] J. H. Wu, J. W. Lei, J. H. Shi, and D. Liu, "The design and simulation of missile internal and external loops with dual PID control," *Applied Mechanics & Materials*, vol. 644-650, pp. 146-149, 2014.
- [10] G. Schweitzer and E. H. Maslen, *Magnetic Bearings: Theory, Design, and Application to Rotating Machinery*. Springer, New York, USA, 2009.



bearings.

Mao Tang was born in 1991. He received B.S. degrees in Mechanical Engineering and Automation from Nanjing University of Aeronautics and Astronautics (NUAA) in 2014. He is currently pursuing a M.S. in NUAA. His research focuses on vibration control and magnetic



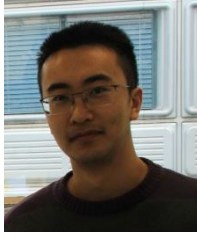
She is currently a Full Professor in the College of Mechanical and Electrical Engineering, Nanjing University of Aeronautics and Astronautics (NUAA). Her research focuses on magnetic bearings and vibration control.

Jin Zhou received the Ph.D. degree in Mechanical Engineering from China University of Mining and Technology (CUMT) in 2001. From 2011 to 2012, she was a Visiting Scholar in the Rotating Machinery and Control Laboratory (ROMAC) of the University of Virginia.



His research focuses on magnetic bearings.

Chaowu Jin obtained B.S., M.S. and Ph.D. degrees in Mechanical Engineering from Nanjing University of Aeronautics and Astronautics (NUAA) from 2002 to 2011. He is currently an Associate Professor in the College of Mechanical and Electrical Engineering, NUAA.



Yuanping Xu was born in 1989. He received B.S. degrees in Mechanical Engineering and Automation from Nanjing University of Aeronautics and Astronautics (NUAA) in 2012. He is currently pursuing a Ph.D. in NUAA and is a guest Ph.D. student in EPFL. His research focuses on magnetic levitation technology.